Journal of Environmental Management 322 (2022) 116166

Contents lists available at ScienceDirect

Journal of Environmental Management

journal homepage: www.elsevier.com/locate/jenvman

Research article

Combining geophysical methods (DC, IP, TDEM and GPR) to characterise mining waste in the Linares-La Carolina district (southern Spain)

J. Rey [a,*], R. Mendoza [b], J. Martínez [b], M.C. Hidalgo [a], C. Florez Rodríguez [b]

[a] Department of Geology, EPS Linares and CEACTEMA, Universidad de Jaén (University of Jaén), Technological Scientific Campus, 23700 Linares, Jaén, Spain
[b] Dept. of Mechanical and Mining Engineering, EPS Linares and CEACTEMA, Universidad de Jaén, Technological Scientific Campus, 23700 Linares, Jaén, Spain

ARTICLE INFO

Keywords:
Mine wastes
Environmental quality
Pollution
Geophysical methods

ABSTRACT

The accumulation of waste materials in old, abandoned mining districts without prior sealing of the substrate currently poses a significant risk of contamination to soils and surrounding waters. Some of these mining dams have undergone a reclamation and sealing process in recent years to alleviate this problem. The current study is an analysis of the effectiveness of using different geophysical techniques for characterising these structures and monitoring the isolation performed. This study was carried out in the old mining district of Linares-La Carolina (southern Spain). The following techniques were investigated in this study: direct current (DC) resistivity, induced polarization (IP), ground-penetrating radar (GPR) and the time domain electromagnetic method (TDEM).

Combining DC and IP made it possible to characterise the internal structure of the abandoned mining dams, whereby the geometry of these deposits was determined and the corresponding potential risks were assessed. In addition, percolation zones of mining leachates were detected that indicate defects in the sealing stage.

TDEM was a good complementary technique for calculating the depth of the bedrock on which the mining dam is located. GPR could only be used to investigate shallow depths at all of the antenna frequencies used (100, 250 and 500 MHz) but was useful for obtained detailed information about the last stages of filling and characterising the encapsulation performed during sealing.

1. Introduction

Very large volumes of waste (waste rock, flotation sludge, smelter slag, etc.) generated in old mining districts have accumulated in the vicinity of the facilities without the implementation of any type of corrective measures. Therefore, these wastes have polluted and, in many cases, continue to pollute the soils and waters of the environment decades after the closure of mining operations (Sobanska et al., 2000; Li and Thornton, 2001; Chopin and Aloway, 2007). Numerous studies performed in different countries on soils and waters affected by mining activities reflect there is a worldwide problem. As an example, Gratton et al. (2000) conducted a study on contamination in old mercury (Hg) mines in the US, Australia, and Canada and detected a large regional impact of metal(oid)s 30 years after mine closure. Of special relevance are studies associated with mining in South America, among which Veado et al. (2006) have reported adverse effects of mining operations on plants and soils more than 400 km away from the original source of contamination in Minas Gerais (Brazil). Numerous studies have been performed in Spain on detecting high concentrations of heavy metals in soils associated with old mining districts, including Río Tinto (Nieto et al., 2007), Almadén (Schmid et al., 2013), Cartagena (García et al., 2001; Acosta et al., 2014) and Linares (Martínez et al., 2008).

Addressing this environmental problem requires characterising the geometry and internal structure of these mining wastes, as well as the sealing of these wastes. Recent years have witnessed efforts towards closure and reclamation of various abandoned deposits produced by treatment processes of extractive industries. Measures have been proposed for the physical and chemical stabilization of deposits to guarantee their long-term structural safety and prevent any type of contamination. Most measures that have carried out have focused on the encapsulation of mining sludge.

Many studies in the literature have shown that indirect (geophysical) methods are useful for characterising former tailings dams in terms of reconstructing the morphology, locating recharge–discharge areas, and

* Corresponding author.
E-mail addresses: jrey@ujaen.es (J. Rey), rmendoza@ujaen.es (R. Mendoza), jmartine@ujaen.es (J. Martínez), chidalgo@ujaen.es (M.C. Hidalgo), cafr0003@red.ujaen.es (C.F. Rodríguez).

https://doi.org/10.1016/j.jenvman.2022.116166
Received 8 May 2022; Received in revised form 17 August 2022; Accepted 31 August 2022
Available online 7 September 2022

identifying points of contact between the substrate and the deposited waste of. The direct current (DC) resistivity method is one of the most frequently used techniques with demonstrated utility for numerous mining districts (Grangeia et al., 2011; Martínez-Pagán et al., 2011; Martín-Crespo et al., 2015; Pierwoła, 2015; Zarroca et al., 2015; Tycholiz et al., 2016; Martínez et al., 2021). This technique has been used in conjunction with induced polarization (IP) to locate leachate and contamination areas (Pierwoła, 2015; Power et al., 2018; Rey et al., 2020; Martínez et al., 2021). Electrical resistivity imaging (ERI) is occasionally used in combination with more superficial methods (ground-penetrating radar, GPR) that gauge the effectiveness of the isolation process to which these structures have been subjected (Poisson et al., 2009; Grangeia et al., 2011; Cortada et al., 2017). The time domain electromagnetic method (TDEM) has been widely used in environmental studies (Kafri and Goldman, 2006; Hu et al., 2016). However, TDEM has rarely been used to characterise mine tailings.

In previous studies, more than two indirect methods are not used for the characterisation of tailings dams. This study was carried out in the old mining district of Linares-La Carolina (in the south of Spain) using DC, IP, GPR and TDEM. The aim of this study was to assess the capacity of these four geophysical methods to characterise the geometry and growth stages of a dam and to determine the type and effectiveness of the encapsulation used. This characterisation can be used to determine the environmental risk posed by mining waste. The evaluation of multiple methods conducted in this study eliminates the uncertainty in interpretation associated with using a single technique, while identifying the strengths and limitations of the individual geophysical techniques. Therefore, our study can be used as a reference for mining regions worldwide.

2. Description of the study area

The Linares-La Carolina metallogenic district (SE Spain, Fig. 1A) is characterised by the presence of philonian deposits that are primarily composed of galena (lead sulfide, PbS) and hosted in a Paleozoic basement. This basement is basically constituted by granites in the Linares sector and quartzite layers alternating with phyllites in the La Carolina sector (Azcárate, 1977; Larrea et al., 1994). The Palaeozoic basement is fossilized by Triassic red sandstones and shales and Quaternary alluvial facies.

This district was intensively exploited for galena and abandoned at the end of the 1970s. A large quantity of waste materials was deposited near the mining operations. In addition, wastes of mineral concentration processes, and in particular, reject material from the flotation-washing plant, were deposited at the study site without any conditioning measures (Figs. 1B, 2A and B).

Leachates generated by regional processes have been reported to contain high contents of sulfates and specific metallic elements as a result of the oxidation of sulfides in the dumps and flotation waste (Hidalgo et al., 2010; Rojas et al., 2019; Mendoza et al., 2020). Processes affecting the surrounding soils have also been described (Martínez et al., 2008).

The waste rock deposits associated with a former flotation-washing plant (Siles Group, Fig. 1A) in the vicinity of Linares were investigated in this study. Several mining dams along the Guadiel River have been preserved in this environment, among which two of were reclaimed in 2012 and one has not been reclaimed. The reclamation project for one of the restored dams, called the Adaro Washery (García-Fernández and Gallego, 2009), employed in situ encapsulation through impermeable barriers, in addition to controlling surface runoff and restoring the vegetation cover. The sludge was sealed by placing a separation barrier between the waste and the surrounding environment. A "sealing" layer was placed vertically on the slopes (from bottom to top), consisting of 30-cm-thick clay, a protective layer (a geotextile) and a 100-cm-thick "covering" layer made of compacted earth and compost (for the upper part of the profile). Subsequent studies were carried out on this dam using GPR (Cortada et al., 2017) to differentiate among the different encapsulations performed during sealing and detect imperfections in the isolating layers and shallow high-humidity areas.

The current study was performed on the other reclaimed dam, which is known as "La Carlota". Fig. 1B shows the dam location on the left bank of the Guadiel River, which is a few metres from the river channel and

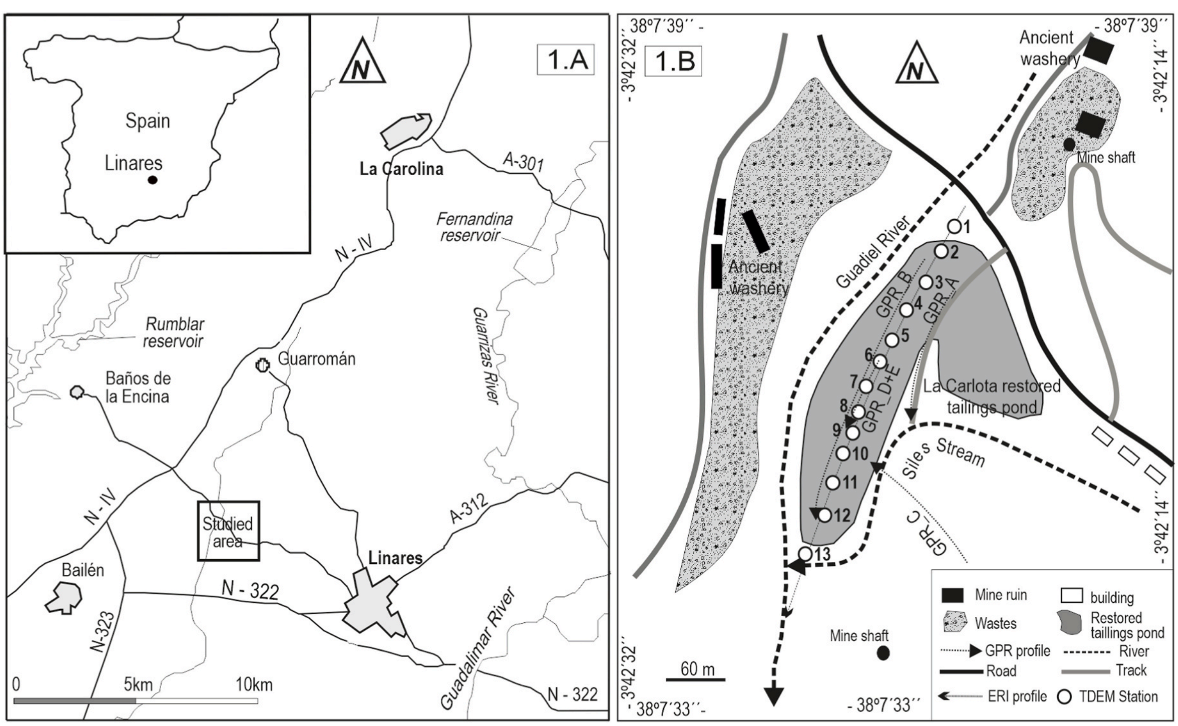

Fig. 1. (A) Geographic location of the studied sector in SE Spain. (B) Position of the La Carlota fines dam in the Siles Group sector. The tomography, GPR, and TDEM station profiles are shown.

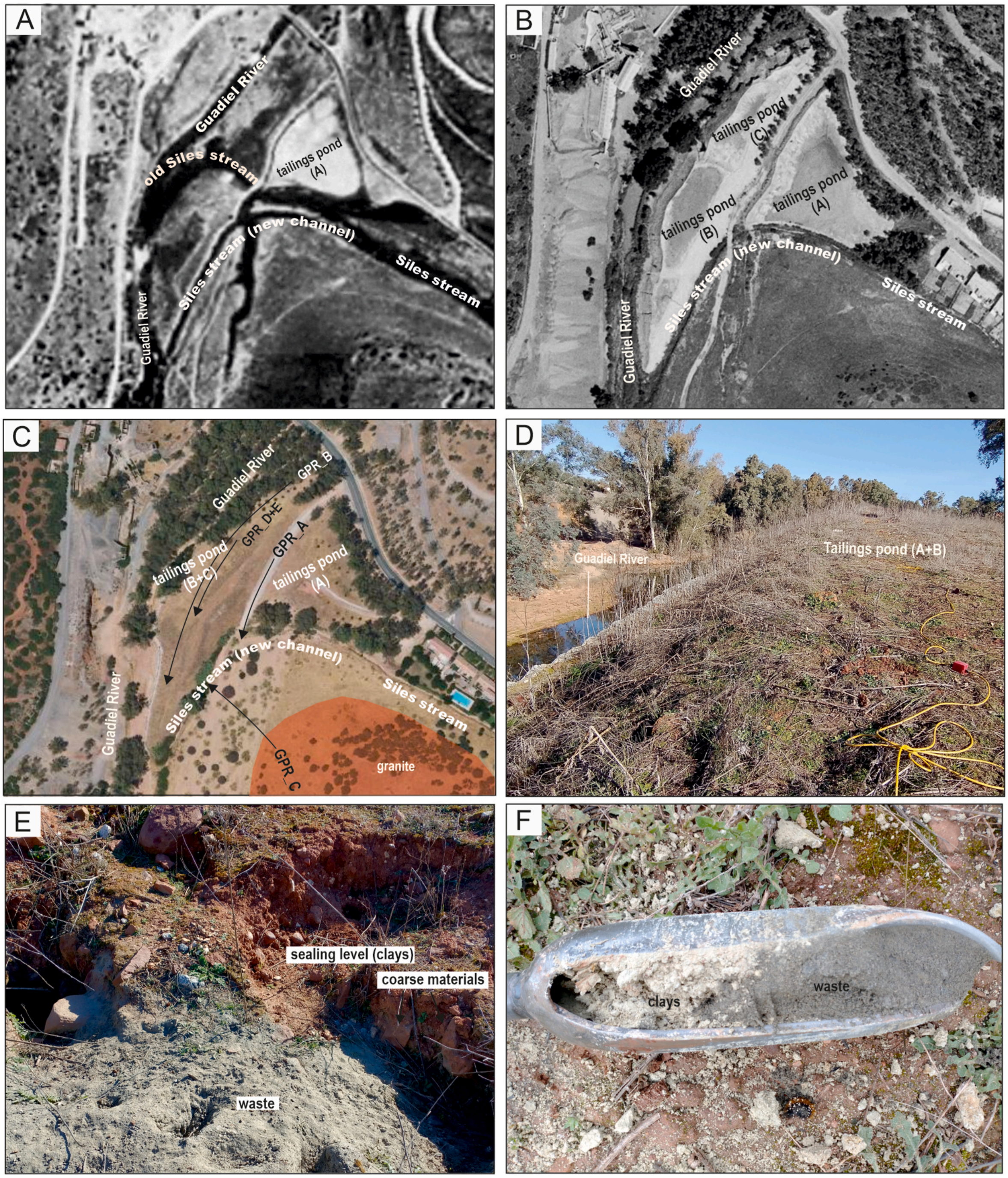

Fig. 2. (A) An aerial photograph taken in 1956, in which the La Carlota sludge pond appears active, already full in the eastern sector (Sector A) and only partially full in the western sector (Sectors B and C). The former channel of the Siles stream can be seen separating these two growth zones from the pond. New channelling of the stream is also observed. (B) An aerial photograph taken between 1973 and 1986 in which the La Carlota sludge pond appears in its terminal stage. Growth of the pond caused Sectors B and C to connect, resulting in the disappearance of the former channel of the stream. The new channelling of the stream enabled the regrowth of Sector A at the southern end of the stream. (C) A current aerial photograph showing the reclaimed sludge pond: the positions of the GPR_A and GPR_C lines are indicated. The photographs 2A, 2B and 2C were extracted from the open access Digital Photo Library of the National Geographic Information Centre of Spain. (D) The electrical tomography profile for the upper area of Sector B, where the Guadiel River is on the left. (E) A detail of the sealing of the slope of the La Carlota pond: a layer of poorly graded red clay appears over the grey mining waste. Sandstone pebbles are evident in this layer of clays in the photograph. (F) The core taken in the upper part of the dam, at the contact between the clays used for isolating the pond and the mining sludge (approximately 50 cm deep). The thickness of the sealing layer and the nonuse of a geotextile for encapsulation are verified. (For interpretation of the references to colour in this figure legend, the reader is referred to the Web version of this article.)

lies directly over unsealed fluvial deposits (Fig. 2. A, 2. B and 2.C). Growth occurred on the fluvial terrace and therefore, on a generally flat surface. The structure was built from a small dike and could therefore grow vertically. The discharge system operated by means of guttering (gravity) from the periphery.

The structure has a maximum length of 260 m, a width between 60 and 160 m and a height of approximately 10–15 m, with an estimated waste volume of approximately 250,000 m^3. The sludge deposits are made up of fine-to medium-grained materials that contain, among other mineral species, Pb sulfides of little economic value that were rejected by the flotation plant and a small proportion of metallic ore particles that were not mined because of poorly developed extractive technology or for being economically unusable (Martínez et al., 2021).

Fig. 2 shows three aerial photographs of these wastes, the first of which was taken in 1956 (Fig. 2A). Three sectors in the pond can be seen. The first sector (A in Fig. 2A) is almost full. The channel of the Siles stream has been modified to regrow Zone A towards the south and increase the discharge zones B and C (as shown in Fig. 2B). The second photograph was taken between 1973 and 1986 (Fig. 2B) and shows the La Carlota sludge pond in its terminal stage. The former channel of the Siles stream has disappeared as a result of connecting Sectors B and C, as well as the expansion of Sector A of the pond towards the south. In the third aerial photograph (Fig. 2C), the reclaimed sludge pond is bounded by the Guadiel River (Fig. 2. D) and the Siles stream.

Although no information is available on the reclamation project for the La Carlota tailings pond, the work done does not appear to have been aligned with the project carried out on the other nearby previously reclaimed dam, the Adaro Washery. The observations of the outcrops (Fig. 2E) and the cores taken show only an approximately 30–50-cm-thick clay "sealing" layer placed directly over the waste (Fig. 2F). Therefore, neither a protective layer (geotextile) nor a 100-cm-thick "cover" layer was used, unlike in the other reclaimed dam. In addition, the granular texture of the clays used is not uniform: there are numerous sandstone pebbles (Fig. 2E).

3. Material and methods

3.1. Direct current resistivity

DC resistivity methods involve determining the distribution of electrical resistivities in subsoil. An electric current is transmitted to the subsurface by two electrodes, and the voltage is monitored using two other electrodes. (Telford et al., 1990). DC resistivity is one of the most effective nondestructive tools for the study and characterisation of subsoil, with emphasis on ERI. This technique consists of implanting numerous electrodes along profiles at a specified distance that is determined by the degree of resolution, depth, and objectives to be achieved: a smaller separation between electrodes increases resolution, whereas a larger separation increases investigation depth (Sasaki, 1992).

DC resistivity has been proven to be useful for reconstructing the morphology of mining dams, locating recharge–discharge areas, and identifying the waste-substrate interface (Martínez-Pagán et al., 2009; Martín-Crespo et al., 2015; Pierwoła, 2015; Zarroca et al., 2015; Tycholiz et al., 2016; Cortada et al., 2017; Martínez et al., 2021).

In this study, a NE−SW direction profile of ERI was run along the sludge pond (Fig. 1B) using 64 electrodes with a 6-m spacing (Fig. 2D) over a total length of 378 m. A Wenner-Schlumberger array was used. This device has an excellent signal-to-noise ratio, both vertically and horizontally, and is therefore very useful for investigating horizontal layers with lateral changes in facies and/or verticalized structures (Dahlin and Zhou, 2004; Loke, 2014).

The following parameters were used to calculate the resistivity: an injection voltage of 800 V, an injection time of 1024 ms, a delay of 10 ms, and a measurement interval of 1000 ms.

A Deutsche Montan Technology (DMT) RESECS was used to perform electrical tomography. After field data acquirement, the dataset must first eliminate anomalous measures by using PROSYSII software. The software was also used to add the terrain topography. The values of the apparent resistivity and chargeability determined in the field study (by IP) were processed using specific RES2DINV software for resistivity and IP data (Griffiths and Barker, 1993). The inversion used a modeling program based on the robust finite element method and a non-linear smoothness-constrained least-squares optimization to produce a model that emphasizes the vertical resistivity features.

3.2. Induced polarization

The IP method consists of measuring a slow voltage decay in the ground following the cessation of an excitation current pulse (Sumner, 1976; Telford et al., 1990). The decline curve is recorded during a prescribed interval, and the area below the curve between two time limits is calculated and then divided by the normal potential Vo as a measure of the time integral of the IP. The resulting value is called the chargeability (Binley and Kemna, 2005; Zhadanov, 2018).

IP has been used in recent years to perform geophysical prospecting in environmental studies (Slater and Lesmes, 2002) for the detection of hydrocarbon polluting plumes (Blondel et al., 2014) or the analysis of industrial waste ponds (Aristodemou and Thomas-Betts, 2000) or leachates in mining dams (Yuval and Oldenburg, 1996; Pierwoła, 2015; Power et al., 2018; Rey et al., 2020).

In this study, a detailed profile centred on the mining dam was obtained (Fig. 3) using 64 electrodes at 6-m intervals over a total length of 378 m and coincided with the aforementioned ERI profile.

A resistivity metre was used to jointly measure the resistivity and apparent chargeability, where nonpolarizing electrodes were used to increase the measurement stability and prevent electrode polarization under prolonged current injection. The metre body was filled with lead chloride saturated in hard gel, into which a lead spiral was cemented. RES2DINV software was also employed to invert IP data.

3.3. Time domain electromagnetic method

The operating principle of TDEM is the circulation of an electric current through a transmitter coil for short periods of time. Abrupt interruption of the current flow causes the primary magnetic field to vary, which induces a variable electric current. This current, in turn, generates a transient secondary magnetic field. The induced currents flow in closed trajectories and migrate to larger depths, thereby decreasing in intensity over time. Changes in the secondary magnetic field over time induce a transient voltage in the receiving coil. The form of the voltage decay provides information on the conductivity distribution in the subsoil, which can be used to characterise the subsoil (Nabighian, 1988; Telford et al., 1990; McNeill, 1994).

This methodology has also been used in environmental studies for the analysis of hydrocarbon polluting plumes (Hu et al., 2016) or the characterisation of marine intrusions (Kafri and Goldman, 2006; Levi et al., 2008).

An ELGEO Research & Production Company AIE-2 was used to perform TDEM in this study. This instrument has a maximum output power of 200 W and a current intensity of up to 10 A. The TDEM receiver is based on a 16-bit analogue-digital converter with a signal processor that provides analogue-to-digital conversion that is impervious to input-voltage noise and real-time signal preprocessing. The instrument has a measurement range between 10 ms and 10 s, with an input voltage between 5 and 20 V with signal compensation.

A total of 13 TDEM measurement stations were installed for the field study and were aligned in the NE−SW direction to coincide with the electrical tomography line. The points in Fig. 2A indicate the centres of the reading stations for square loops of 20 $\times$ 20 m and of 10 $\times$ 10 m on each side (with two turns in this case). Measurements were taken at each point using single loop devices, and the measurement parameters (the intensity, time, voltage) were varied to compare the effectiveness of the different arrays. Different values of the injection amperage (2 A and 5A), voltage (1 V and 10 V), and measurement time (10 ms and 20 ms) were used at each station to identify the most stable curves. In each test, the ramp time was directly proportional to the loop size and amperage used (Christiansen et al., 2009). Given the small size of the loops and technical specifications of the equipment used in this study, a very small ramp time of approximately 2–3 μs was used. A 6-mm^2 section cable was

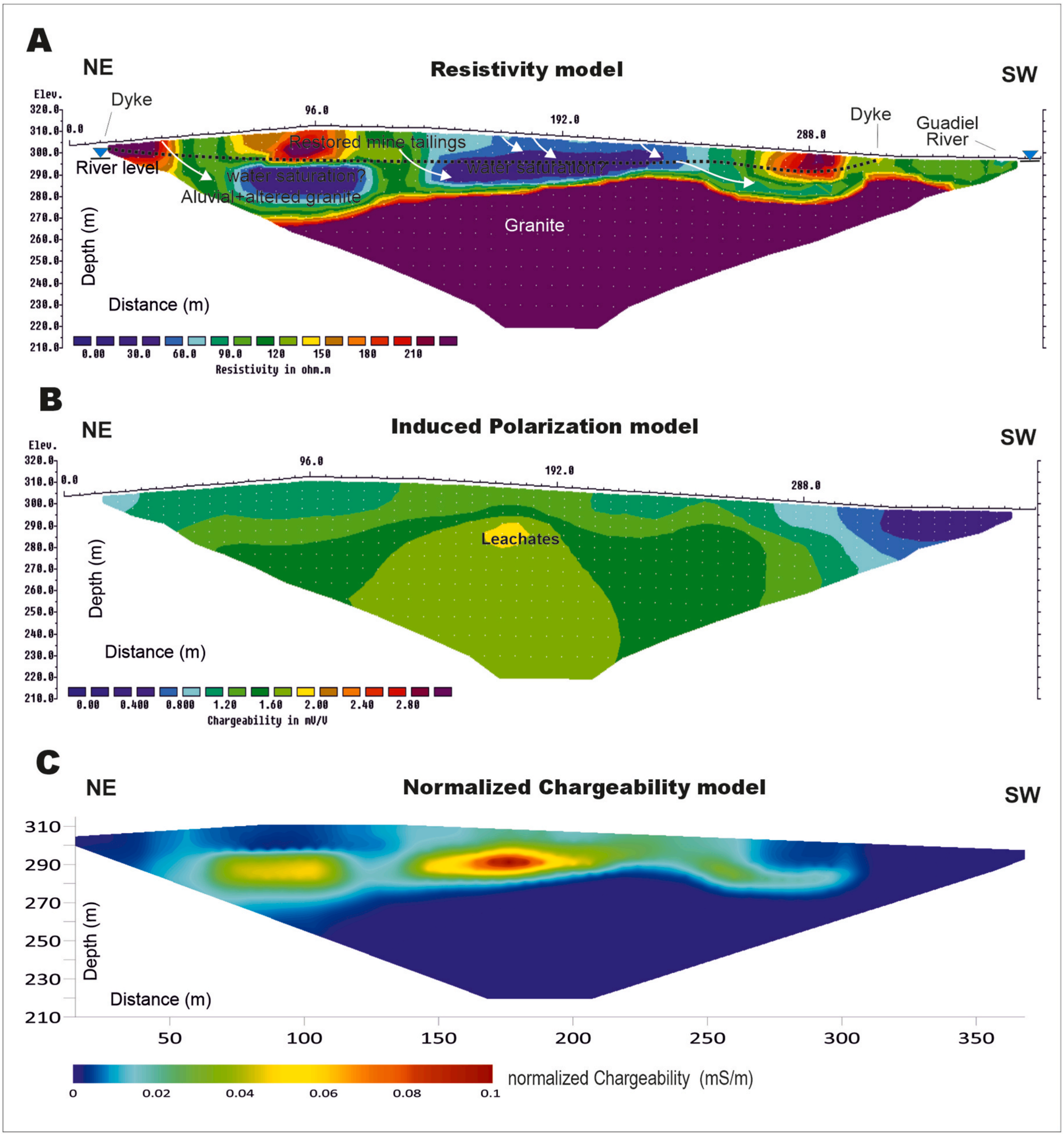

Fig. 3. (A) Resistivity profile, in which the base of the mining waste is indicated by a dashed line. (B) IP profile. (C) Normalized IP profile.

used to reduce the resistance and thereby produce a higher current intensity. TEMBIN software was used to visualise and edit the different curves. The modeling and inversion process was performed with the ZondTEM1D programme.

3.4. Ground-penetrating radar

GPR methods are based on the propagation of high-frequency (between 20 MHz and 1 GHz) electromagnetic waves in a domain in subsoil. The equipment used includes a transmitting antenna that is moved along the ground surface and emits temporary impulses of very short duration. Upon encountering dielectric contrast in the subsoil, these waves are reflected towards the surface, where their characteristics are measured by a receiving antenna (Auken et al., 2003). The penetration depth and resolution depend on the electromagnetic properties of the scanned materials and the antenna used. Thus, an increase in the ground conductivity or the frequency of the transmitted signal produces a decrease in the intensity of wave propagation in the subsoil. For the same profile, the use of high-frequency antennas increases the resolution and decreases the penetration depth, and the opposite result is obtained by decreasing the antenna frequency (Davis and Annan, 1989).

A RAMAC/GPR Pro-Ex model from MALA GEOSCIENCE was used to carry out these studies. The obtained profiles coincided with those obtained using ERI and were accompanied by short perpendicular profiles for the path that joining Sectors A and B + C, as well as for the alluvial deposit adjacent to the Siles stream (Fig. 1B). A total of 19 profiles were obtained, of which only five are discussed in this paper as being the most representative. In all cases, different shielded antennas of 100, 250 and 500 MHz were used. The high-frequency antennas were used to assess the isolation efforts carried out in the dam. The low-frequency antennas were used to determine the internal structure of the sludge. Signal filtering and interpretation were carried out via the Reflexw programme. Different processing tools were applied to the radargrams obtained in the field, for both filtering and gain, as has been performed by other authors (Neal, 2004; Alcalá et al., 2021).

4. Results and discussion

4.1. Direct current resistivity

Data inversion was performed using a total of four iterations, resulting in a root-mean-square (RMS) error of 7%. The resulting resistivity profile is represented in Fig. 3A. Two sets can be differentiated in the vertical direction, of which one set is more superficial, with low-medium values (below 220 Ωm, except at the NE end) associated with the waste in sludge dams, alluvial sands and gravels or highly altered granite. The second set in the lower part of the profile is characterised by increasing resistivity values (which can exceed 1000 Ωm) associated with relatively unaltered granite.

An increase in the resistivity was detected at the two ends of the dam (at 10 m and 320 m from the origin, see Fig. 3A), which corresponds to the peripheral dikes used for the regrowth of the waste dam.

In this type of dam, it is often difficult to use electrical behaviour to differentiate the mining waste from the underlying alluvial materials. However, the sludge resistivity is typically higher (between 60 and 220 Ωm) than that of the of the underlying alluvial deposit (20–110 Ωm). The data obtained from the observations of the outcrops and the vertical changes in resistivities were used to estimate that the base of this body is subhorizontal (Fig. 3A) with maximum thicknesses of approximately 16 m (conditioned by the vertical regrowth). The position of the body is shown in Fig. 3A.

Lateral changes in the resistivity of the mining waste were detected. The resistivity decreases considerably (by as much as 50 Ωm) between 40 and 60 m and between 140 and 240 m from the origin. As described for other sectors, these decreases could be associated with increases in the waste moisture content caused either by percolation of surface water (Rey et al., 2020) or by connection with the Guadiel River.

The resistivity was also found to decrease in the underlying alluvial materials, dropping to 20 Ωm (between 70 and 110 m and between 150 and 220 m from the origin). This decrease could be attributed to the presence of leachates, indicating that the sludge sealing process was not as effective as desired. The presence of leachates in this area was confirmed by IP, as discussed in the next section.

There is a remarkable coincidence between the minimum resistivity associated with alluvial materials between 150 and 220 m from the origin of the profile and that of the former channel of the Siles stream (Fig. 2A). IP can also be used to locate these ancient hidden sedimentary geometries, which are probably saturated with water as a result of being at a lower elevation than the Guadiel River (Fig. 3A).

However, the changes observed in the resistivity sections are associated with uncertainty because they could be caused by different factors: lithological variations in the explored section, variations in water saturation, or changes in the concentration of salts currently in the water. Therefore, chargeability measurements and the calculation of the normalized chargeability section must be performed. This additional information can be used to identify the nature of the observed electrical effects (Slater and Lesmes, 2002; Power et al., 2018).

4.2. Induced polarization (IP)

The trace of the IP profile (Fig. 3B) coincides with that of the resistivity profile shown in Fig. 3A. In this case, four iterations were performed, with a final RMS error of 1.4% for the data inversion process. The chargeability values tend to be low throughout the profile. The chargeability values of the materials in the upper part of the profile (that is, those associated with the pond and the underlying alluvial deposits) do not exceed 1.2 mV/V. The magnitude of the chargeability values shows that the waste material does not contain significant quantities of reactive minerals.

The chargeability values of the underlying granite tend to be low (on the order of 1.5 mV/V), which is common for granitic rocks. No correlation is detected between the first decrease in resistivity (between 70 and 110 m from the origin) and the increase in chargeability. The chargeability values are high, on the order of 2.5–3 mV/V, in only two sectors. These two anomalies appear downstream of the dam and below the elevation of the Guadiel River, at the contact between the alluvial material and granite. The first anomaly occurs between 160 and 180 m from the origin and corresponds to the minimum resistivity zone associated with the former channel of the Siles stream. The second anomaly occurs between 250 and 260 m from the origin and is also located in the underlying alluvial deposit in contact with the granite. The high chargeability in this case should be correlated with low resistivity values. These anomalies cannot be explained in terms of variations in the concentration of sulfides in this dam because the sulfide concentrations are very uniform (García-Fernández and Gallego, 2009; De la Torre et al., 2012). These anomalies could be related to the presence of local filtration. The absence of an increase in the chargeability between 70 and 110 m from the origin could be explained by the lack of a pelitic proportion in the alluvial deposit, probably due to water-saturated sands.

However, it is difficult to determine whether the variations in the IP are caused by the lithology (clayey intercalations in alluvial materials) or effects produced by the pores being saturated by mineralized water. Therefore, some authors have used the normalized chargeability to identify the cause of variations in the IP (Slater and Lesmes, 2002; Blondel et al., 2014; Power et al., 2018). This parameter is the ratio between the chargeability and resistivity.

Fig. 3C shows the normalized chargeability model. The normalized chargeability values are always very low, generally below 0.04 mS/m. The prominent sharp decrease in the normalized chargeability at larger depths is associated with the bedrock (granite). The high resistivities of unaltered granite (see Fig. 3A) correlate very well with the very low normalized chargeability values presented in Fig. 3C.

The normalized chargeability values are slightly elevated in three areas. These three zones are always associated with the alluvial base below the Guadiel River, and the normalized chargeability values coincide with the minimum resistivity values in all zones. The first zone lies between 70 and 110 m, the second zone lies between 160 and 180 m (the former channel of the Siles stream), and the third zone lies between 250 and 260 m from the origin of the profile. The normalized chargeability values in these areas are higher than in other areas but still low (below 0.1 mS/m). The low resistivity values associated with the low normalized chargeability values in these three sectors of the profile are a characteristic response of areas saturated with contaminated water, as has been shown in different field and laboratory studies (Slater and Lesmes, 2002; Power et al., 2018). In our case, the presence of a fluid with a significant load of metallic elements could explain a moderate increase in chargeability in alluvial materials.

The filtration detected between 160 and 180 m and between 250 and 260 m may be related to degradation of the sealing liner.

4.3. Time domain electromagnetic method (TDEM)

Comparing the curves obtained using the 10 × 10 m and 20 × 20 m loops at each station shows that higher stability was obtained using the 20 × 20 m loops. Therefore, the curves obtained using the 20 × 20 m loops are discussed in this section. The RMS error in the interpretation curves of the 13 stations varies but remains within the 3–4.5% range.

In general, a low-resistivity surface set is detected in the curves associated with mining waste, alluvial deposits, and altered granite. Under this set, a resistive body between 12 and 20 m deep, depending on the station, is detected that is associated with the granite. The most representative information obtained for the four stations is analysed here.

Fig. 4A shows the geological model on which the pond is located constructed using the information obtained by electrical prospecting. However, the device used to collect the electrical data cast shadows at both ends of the profile, as can be seen in figure. A highly trafficked road prevented better centring of the profile device, resulting in a lack of information for the NE end of the pond.

This lack of information was compensated for using the TDEM data. Fig. 4B shows the information obtained for the two stations at the NE end (1 and 2) corresponding to the locations shown in Figs. 1B and 4A. Fig. 4B shows the measured induced voltage curves (blue line), the apparent resistivity curves obtained as a function of time (red line), and the resistivity model generated by the inversion software (thick red line). The field line and the result produced by the ZONDTEM1D software model are almost coincident for each curve.

At Station 1, the first layer is approximately 16 m thick and has a low resistivity potential associated with the alluvial deposits. Under this set, an increase in resistivity associated with granite is detected. At the second station, there is a very superficial resistive layer (Fig. 4B) related to the grown dike of the dam. Under the resistive layer are conductive materials (alluvial deposits) with thicknesses of approximately 10 m that are lower than those at the previous station.

This technique cannot be used to differentiate mining waste from the underlying alluvial deposit because the corresponding conductivities are similar. However, at the points at which the thickness of the dam is known (from field data or old aerial photographs), this method can be used to identify underlying granite and therefore the thickness of the alluvial deposit. One example is the alluvial deposit at Station 6, which has a low thickness where the mining waste practically rests on top of the granite (Fig. 4). This result can be confirmed by the ERI profile data. In the case of Station 11 (also shown in Fig. 4B), a deep resistive layer is detected at 23 m. Considering 10-m-thick wastes are based on the measured data for the outcrop, thicknesses of approximately 13 m for the alluvial deposits can be deduced.

4.4. *Ground-penetrating radar*

Fig. 5 shows three of the profiles obtained using the 100-MHz antenna. The GPR_A profile was obtained for the road currently separating Sectors A and B + C of the La Carlota mining dam (the road location is indicated in Fig. 2C). The reflection hyperbolas were analysed using Relexw software to obtain estimated wave velocities of 0.117 m/ns in these lithologies, which are similar to those reported for equivalent materials in other sectors (Poisson et al., 2009; Grangeia et al., 2011; Cortada et al., 2017). Despite the low antenna frequency, the signal is lost at a depth of 3–4 m because the high conductivity of this mining waste rapidly attenuates the wave with increasing depth (Neto and Medeiros, 2006; Takahashi et al., 2011). There are two notable aspects of this first profile (Fig. 5A). First, filling of a depressed area is observed between 0 and 50 m from the origin. Comparing Fig. 2A and B show that this geometry corresponds to the grading of the slopes between Sectors C and B of the mining pond, which lies directly over the former channel of the Siles stream. Prograding geometries towards the SW are observed from 75 m to the end of the profile. These layers correspond to the last growth phases of the pond once the Siles stream was redirected.

The 100-MHz antenna was used to obtain the GPR_B profile for the reclaimed pond (Fig. 5B). The most responsive area is in the section between 70 m and 160 m from the origin. This area corresponds exactly to the sector between Sectors B and C of the dam that developed during the last stage of growth (the location of this sector is shown in Fig. 4A). The third georadar profile was obtained using a 100-MHz antenna placed adjacent to the mining dam on the alluvial deposit associated with the Siles stream (Fig. 5C). The antenna position is shown in Figs. 1B and 2C. The use of this technique enabled the detection of channelised geometries in this sedimentary medium, as well as the contact with the granite associated with the Palaeozoic basement.

To analyse the reclamation process of the dam, higher-frequency antennas (250 MHz and 500 MHz) were used that achieved higher resolution for a lower penetration depth. The location of the respective profiles is shown in Figs. 1B and 4A. A 250-MHz antenna was used to obtain the GPR_D profile (Fig. 5D). In this case, the penetration depth does not usually exceed 1.5 m. The section shown in Fig. 5D coincides with the edge of Sector B of the dam, enabling visualisation of the original slopes of the edge of the structure. Use of this antenna revealed the sealing layer, which is approximately 50–70 cm thick and basically constituted by clayey facies (taken from the Triassic facies outcropping in the vicinity). This layer appears to be perfectly continuous at the frequency used. The amplitude contrasts of the wave correspond to the different compaction layers of these clays.

The 500-MHz antenna has a lower penetration capacity than the 250-MHz antenna. Fig. 5E shows that the penetration depth of the 250-MHz antenna barely exceeds a metre. However, use of the 250-MHz antenna

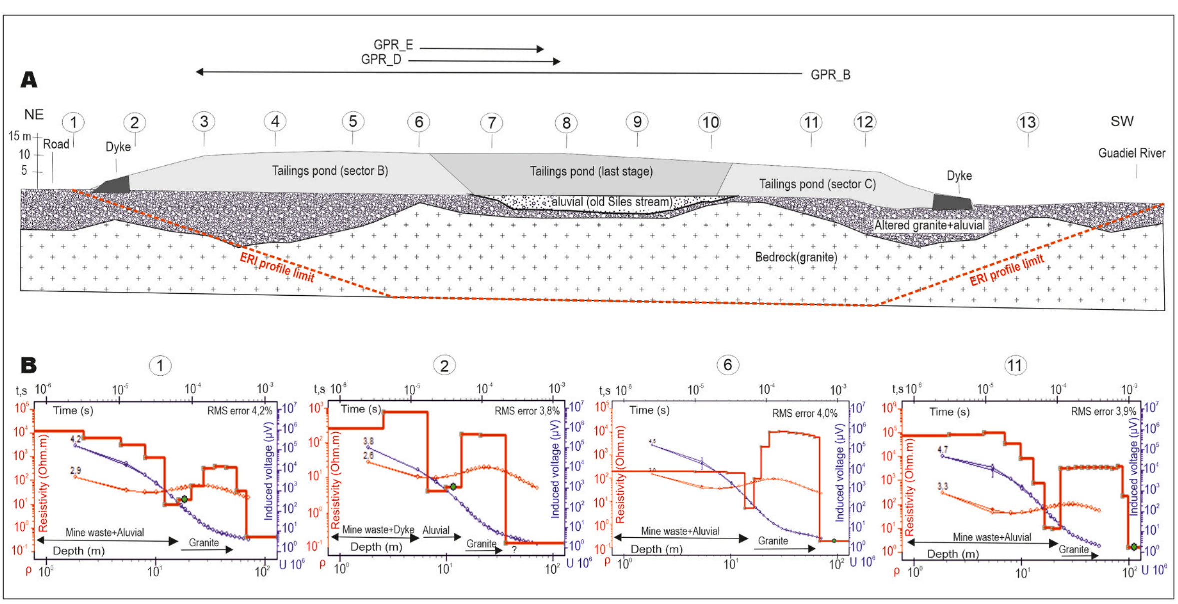

Fig. 4. (A) Section deduced from the information in the ERI profile. The numerals 1, 2, 3 ….13 denote the positions of the TDEM stations. The locations of the three GPR profiles analysed in this study that appear in Fig. 5 (GPR_B, GPR_D, and GPR_E) are also indicated. (B) Graphs showing the TDEM results at four of these stations: the induced voltage curves (blue line) and apparent resistivity (red line) as a function of time are shown. The fits to the field lines by the model (using ZONDTEM1D software) are shown for each curve. The interpretation after data inversion is also included, where the red straight lines represent the resistivity as a function of the depth. (For interpretation of the references to colour in this figure legend, the reader is referred to the Web version of this article.)

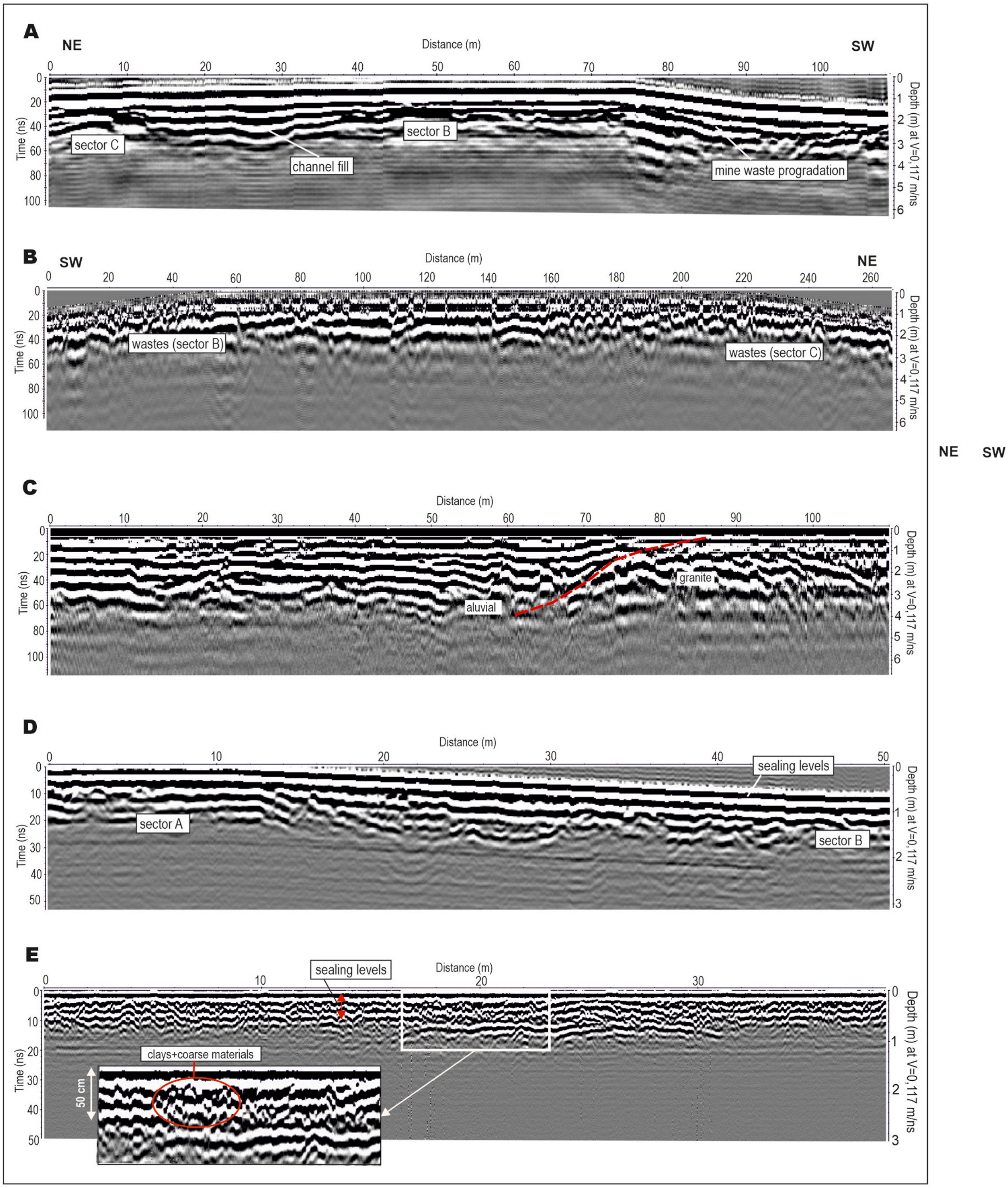

Fig. 5. Details of the GPR profiles obtained using a 100-MHz antenna (A, B, and C). Details of the GPR profile obtained using a 250-MHz antenna (D). Details of the GPR profile obtained using a 500-MHz antenna (E). The antenna locations are shown in Fig. 1B and described in the text.

provided many details on the type of encapsulation. First, the thickness of the respective layer is not constant and varies between 40 and 70 cm. Second, the radargram indicates that the clay layers do not provide good lateral continuity, which is related to laterally uneven compaction. Third, a detailed analysis of Fig. 5E shows innumerable hyperbolas within this layer of sealing. These responses correspond to the sandstone pebbles embedded in the clays, as can also be observed in the outcrop (Fig. 2E). All these results facilitate the identification of defects formed during the encapsulation process.

5. Conclusions

A combination of geophysical prospecting methods were applied in this study for the monitoring of mining dams, both in terms of characterising the dam structure and the subsequent sealing process. The ERI technique was demonstrated to be able to reconstruct the dam morphology, thereby identifying where the waste contacts the substrate.

TDEM was used as a complementary method to the DC resistivity. TDEM could not be used to identify the contact between the waste and the underlying alluvial materials. However, TDEM could be used to detect the depth of the bedrock (granite) under the sedimentary cover and to obtain information of interest at the extremes of the ERI profile where shadow areas were generated.

Decreases in the resistivity values were detected under the waste in the alluvial materials. These low resistivities may indicate the presence of contaminated water below the waste or may result from an increase in the quantity of clayey facies in the alluvial.

Electrical methods, such as DC, IP and normalized IP, were combined to remove this limitation. Thus, areas of low resistivity, high chargeability and a weak increase in the normalized IP were detected in the alluvial deposit under the dam, which are associated with saturation with contaminated water (a fluid with a significant load of metallic elements).

In turn, decreases in resistivity in the dam were detected in the vertical direction for these anomalies and interpreted as resulting from increases in the humidity.

GPR did not penetrate to more than 3–4 m for any of the antennas used (100, 250 and 500 MHz). This result was due to the nature of the sediments, which cause rapid attenuation of the signal. Nevertheless, considerable information was obtained using the lowest frequency antenna (100 MHz) for the first 4 m and therefore, of the last growth stages of these mining structures. The higher-resolution (but lower penetration) 500-MHz antenna could characterise the encapsulation phases the mining dam was subjected to during the sealing and reclamation stage. The seal thickness, lateral continuity, and uniformity of the rock used were detected. In our study, we detected changes in the thickness and differential compaction of the clay and the presence of an inadequate granular texture (abundant sandstone pebbles within the clay layer).

Failure to isolate the structure during sealing (as detected by GPR) may have enabled the increase in humidity in the dam and the percolation of contaminated water through the underlying alluvial facies.

Author contribution

Javier Rey: investigation. Software and data curation. Writing-Original draft preparation. RosendoMendoza: investigation. Software and data curation. Julián Martínez: investigation. Software and data curation. Carmen Hidalgo: Conceptualization, Reviewing. Camilo Florez: Investigation.

Declaration of competing interest

The authors declare the following financial interests/personal relationships which may be considered as potential competing interests: Javier Rey reports financial support was provided by University of Jaen. Javier Rey reports financial support was provided by Junta de Andalucía, Spain.

Data availability

Data will be made available on request.

Acknowledgements

This study was funded by the FEDER Andalucía R&D Project (Grant No. 1380520) and the University of Jaen (Spain). Careful reviews of the manuscript by anonymous referees substantially improved the manuscript.

References

Acosta, J.A., Martínez-Pagán, P., Martínez-Martínez, S., Faz, A., Zornoza, R., Carmona, D. M., 2014. Assessment of environmental risk of reclaimed mining ponds using geophysics and geochemical techniques. J. Geochem. Explor. 147, 80–90. https://doi.org/10.1016/J.GEXPLO.2014.04.005.

Alcalá, F.J., Martínez-Pagán, P., Paz, M.C., Navarro, M., Pérez-Cuevas, J., Domingo, F., 2021. Combining of MASW and GPR imaging and hydrogeological surveys for the groundwater resource evaluation in a coastal urban area in southern Spain. Appl. Sci. 11, 3154. https://doi.org/10.3390/app11073154.

Auken, E., Jørgensen, F., Sørensen, K.I., 2003. Large-scale TEM investigation for groundwater. Explor. Geophys. 34, 188–194.

Aristodemou, E., Thomas-Betts, A., 2000. DC resistivity and induced polarisation investigations at a waste disposal site and its environments. J. Appl. Geophys. 44, 275–302.

Azcárate, J.E., 1977. Mapa geológico y memoria explicativa de la hoja 905 (Linares), escala 1:50.000. Instituto Geológico y Minero de España.

Binley, A., Kemna, A., 2005. DC resistivity and induced polarization methods. In: Rubin, Y., Hubbard, S.S. (Eds.), Hydrogeophyiscs. Springer-Verlag.

Blondel, A., Schmutz, M., Franceschi, M., Tichané, F., Carles, M., 2014. Temporal evolution of the geoelectrical response on a hydrocarbon contaminated site. J. Appl. Geophys. 103, 161–171.

Cortada, U., Martínez, J., Rey, J., Hidalgo, M.C., 2017. Assessment of tailings pond seals using geophysical and hydrochemical techniques. Eng. Geol. 223, 59–70. https://doi.org/10.1016/j.enggeo.2017.04.024.

Chopin, E.I.B., Aloway, B.J., 2007. Trace element partitioning and soil particle characterization around mining and smelting areas at Tharsis, Ríotinto and Huelva, SW Spain. Sci. Total Environ. 373, 488–500.

Christiansen, A.V., Auken, E., Sorensen, K., 2009. The transient electromagnetic method. In: Kirsch, R. (Ed.), Groundwater Geophysics, a Tool for Hydrogeology. Springer, pp. 179–224.

Dahlin, T., Zhou, B., 2004. A numerical comparison of 2D resistivity imaging with 10 electrode arrays. Geophys. Prospect. 52, 379–398.

Davis, J.L., Annan, A.P., 1989. Ground-penetrating radar for high-resolution mapping of soil and rock stratigraphy. Geophys. Prospect. 37, 531–551.

De la Torre, M.J., Hidalgo, M.C., Rey, J., Martínez, J., 2012. Mineralogical characterization of tailing dams: 372 incidence of abandoned mining works on soil pollution (Linares, Jaén). Geophysical Research 373, 14. Abstracts.

García, M.M., Moreno-Grau, S., García, J.M., Moreno, J., Bayo, J., Perez, J.G., Moreno-Clavel, J., 2001. Distribution of the metals lead, cadmium, copper, and zinc in the top soil of Cartagena, Spain. Water Air Soil Pollut. 131, 329–347.

García-Fernández, J.M., Gallego, J., 2009. Proyecto de clausura y restauración del depósito de procesos d tratamiento de industrias extractivas abandonado "0905-2-0002". EGMASA, Consejería Medio Ambiente, Junta de Andalucía (unpublished).

Grangeia, C., Ávila, P., Matias, M., Ferreira da Silva, E., 2011. Mine tailings integrated investigations: the case of Rio tailings (Panasqueira Mine, Central Portugal). Eng. Geol. 123, 359–372.

Gratton, W.S., Nkongolo, K.K., Spiers, G.A., 2000. Heavy metal accumulation in soil and Jack pine (pinus Banksiana) needles in Sudbury, Ontario, Canada. Bull. Environ. Contam. Toxicol. 64, 550–557.

Griffiths, D.H., Barker, R.D., 1993. Two-dimensional resistivity imaging and modelling in areas of complex geology. J. Appl. Geophys. 29, 211–226.

Hidalgo, M.C., Rey, J., Benavente, J., Martínez, J., 2010. Hydrogeochemistry of abandoned Pb sulphide mines: the mining district of La Carolina (southern Spain). Environ. Earth Sci. 61, 37–46.

Hu, Y., Zeng, Z., Chen, X., Zhao, X., 2016. Application of Transient Electromagnetic Method in saturation region detection in tailings dam. 7th International Conference on Environmental and Engineering Geophysics & Summit Forum of Chinese Academy of Engineering on Engineering Science and Technology 318–321. Atlantis Press.

Kafri, U., Goldman, M., 2006. Are the lower subaquifers of the Mediterranean coastal aquifer of Israel blocked to seawater intrusion? Results of a TDEM (time domain electromagnetic) study. Isr. J. Earth Sci. 55, 55–68.

Larrea, F.J., Carracedo, M., Ortega Cuesta, L., Gil Ibarguchi, J.I., 1994. El Plutón de Linares (Jaén): cartografía, petrología y geoquímica. Cuaderno Laboratorio Xeológico de Laxe Coruña 19, 335–346.

Levi, E., Goldman, M., Hadad, A., Gvirtzman, H., 2008. Spatial delineation of groundwater salinity using deep time domain electromagnetic geophysical measurements: a feasibility study. Water Resour. Res. 44, W12404 https://doi.org/10.1029/2007WR006459.

Li, X., Thornton, I., 2001. Chemical partitioning of trace and mayor elements in soils contaminated by mining and smelting activities. Appl. Geochem. 16, 1693–1706.

Loke, M.H., 2014. Tutorial: 2-D and 3-D Electrical Imaging Surveys. Revision date: 5th November 2014. www.geotomosoft.com. accessed 2015-02-19).

McNeill, J.D., 1994. Principles and Application of Time Domain Electromagnetic Techniques for Resistivity Sounding. Geonics Ltd, Ontario. Technical Note TN-27. http://www.geonics.com/pdfs/technicalnotes/tn27.pdf.

Martínez, J., Llamas, J.F., De Miguel, E., Rey, J., Hidalgo, M.C., 2008. Soil contamination from urban and industrial activity: example of the mining district of Linares (southern Spain). Environ. Geol. 54, 669–677.

Martínez, J., Mendoza, M., Rey, J., Sandoval, S., Hidalgo, M.C., 2021. Characterization of tailings dams by electrical geophysical techniques (ERT, IP): federico Mine (La Carolina, southeastern Spain). Minerals 11, 145. https://doi.org/10.3390/min1102014.

Martín-Crespo, T., Gómez-Ortíz, D., Martín-Velázquez, S., Esbrí, J.M., De Ignacio-San José, C., Sánchez-García, M.J., Montoya-Montes, I., Martín-González, F., 2015. Abandoned mine tailings in cultural itineraries: don Quixote route (Spain). Eng. Geol. 197, 82–93.

Martínez-Pagán, P., Faz Cano, A., Aracil, E., Arocena, J.M., 2009. Electrical resistivity imaging revealed the spatial properties of mine tailing ponds in the sierra minera of southeast Spain. J. Environ. Eng. Geophys. 14, 63–76.

Martínez-Pagán, A., Faz, J.A., Acosta, D.M., Carmona, S., Martínez-Martínez, A., 2011. A multidisciplinary study for mining landscape reclamation: a study case on two tailing ponds in the Region of Murcia (SE Spain). Phys. Chem. Earth 36, 1331–1344. https://doi.org/10.1016/j.pce.2011.02.007.

Mendoza, R., Martínez, J., Rey, J., Hidalgo, M.C., Campos-Suñol, M.J., 2020. Metal(loid)s transport in Hydrographic networks of mining basins: the case of the La Carolina mining district (Southeast Spain). Geosciences 10, 391. https://doi.org/10.3390/geosciences101100391.
Nabighian, N.M., 1988. Electromagnetic Method in Applied Geophysics. Tulsa, Okla. Society of Exploration Geophysics, p. 971.
Neal, A., 2004. Ground-penetrating radar and its use in sedimentology: principles, problems and progress. Earth Sci. Rev. 66, 261–330.
Neto, P.X., Medeiros, W.E., 2006. A practical approach to correct attenuation effects in GPR data. J. Appl. Geophys. 59, 140–151.
Nieto, J.M., Sarmiento, A.M., Olías, M., Cánovas, C.R., Riba, I., Kalman, J., Angel Delvalls, T., 2007. Acid mine drainage pollution in the Tinto and odiel rivers (iberian pyrite belt, SW Spain) and bioavailability of the transported metals to the huelva estuary. Environ. Int. 33, 445–455.
Pierwoła, J., 2015. Using geoelectrical imaging to recognize Zn-Pb post-mining waste deposits. Pol. J. Environ. Stud. 24, 2127–2137. https://doi.org/10.15244/pjoes/43498.
Poisson, J., Chouteau, M., Aubertin, M., Campos, D., 2009. Geophysical experiments to image the shallow internal structure and the moisture distribution of a mine waste rock pile. J. Appl. Geophys. 67, 179–192.
Power, Ch, Tsourlos, P., Ramasamy, M., Nivorlis, A., Mkandawire, M., 2018. Combined DC resistivity and induced polarization (DC-IP) for mapping the internal composition of a mine waste rock pile in Nova Scotia, Canada. J. Appl. Geophys. 150, 40–51.
Rey, J., Martínez, J., Hidalgo, M.C., Mendoza, R., Sandoval, S., 2020. Assessment of tailings ponds by a combination of electrical (ERT and IP) and hydrochemical techniques (Linares, southern Spain). Mine Water Environ. 40 https://doi.org/10.1007/s10230-020-00709-3.
Rojas, D., Hidalgo, M.C., Kohfahl, C., Rey, J., Martínez, J., 2019. Oxidation dynamics and composition of the flotation plant derived tailing impoundment Aquisgrana (Spain). Water Air Soil Pollut. 230 (7) https://doi.org/10.1007/s11270-019-4190-1.
Sasaki, Y., 1992. Resolution of resistivity tomography inferred from numerical simulation. Geophys. Prospect. 40, 453–464.
Schmid, Th, Rico, C., Rodríguez-Rastrero, M., Sierra, M.J., Díaz-Puente, M.J., Pelayo, M., Millán, R., 2013. Monitoring of the mercury mining site Almadén implementing remote sensing technologies. Environ. Res. 125, 92–102.
Slater, L., Lesmes, D., 2002. IP interpretation in environmental investigations. Geophysics 67, 77–88. https://doi.org/10.1190/1.1451353.
Sobanska, S., Ledésert, B., Deneele, D., Laboudigue, A., 2000. Alteration in soils of slag particles resulting from lead smelting. Comptes Rendus Académie des Sciences-Paris Série IIA- Earth and Planetary Science 331, 271–278.
Sumner, J.S., 1976. In: Principes of Induced Polarization for Geophysical Exploration. Elsevier Scientific Publishing, Amsterdam, p. 277.
Takahashi, K., Preetz, H., Igel, J., 2011. Soil properties and performance of landmine detection by metal detector and ground-penetrating radar — soil characterisation and its verification by a field test. J. Appl. Geophys. 73, 368–377.
Telford, W.M., Geldart, L.P., Sheriff, R.E., 1990. Applied Geophysics. Cambridge University Press, p. 770.
Tycholiz, C., Ferguson, I.J., Sherriff, B.L., Cordeiro, M., Sri Ranjan, R., Pérez-Flores, M.A., 2016. Geophysical delineation of acidity and salinity in the Central Manitoba gold mine tailings pile, Manitoba, Canada. J. Appl. Geophys. 131, 29–40. https://doi.org/10.1016/j.jappgeo.2016.05.006.
Veado, M.A., Arantes, I.A., Oliveira, A.H., Almeida, M.R., Miguel, M.I., Severo, M.I., Cabaleiro, H.L., 2006. Metal pollution in the environment of Minas Gerais state – Brazil. Environ. Monit. Assess. 117, 157–172.
Yuval, Z., Oldenburg, D.W., 1996. DC resistivity and IP methods in acid mine drainage problems: results from the Copper Cliff mine tailings impoundments. J. Appl. Geophys. 34, 187–198.
Zhadanov, M.S., 2018. Direct current and induced polarization methods. In: Foundations of Geophysical Electromagnetic, Theory and Methods. Elsevier, pp. 439–493.
Zarroca, M., Linares, R., Velásquez-López, P.C., Roqué, C., Rodríguez, R., 2015. Application of electrical resistivity imaging (ERI) to a tailings dam project for artisanal and small-scale gold mining in Zaruma-Portovelo, Ecuador. J. Appl. Geophys. 113, 103–113.